Cell Death and Differentiation (2014) 21, 797–810

www.nature.com/cdd

Isthmin targets cell-surface GRP78 and triggers apoptosis via induction of mitochondrial dysfunction

M Chen[1], Y Zhang[1], VC Yu[2], Y-S Chong[3], T Yoshioka[4] and R Ge*[,1]

Isthmin (ISM) is a secreted 60-kDa protein that potently induces endothelial cell (EC) apoptosis. It suppresses tumor growth and angiogenesis in mice when stably overexpressed in cancer cells. Although $\alpha v\beta 5$ integrin serves as a low-affinity receptor for ISM, the mechanism by which ISM mediates antiangiogenesis and apoptosis in ECs remain to be fully resolved. In this work, we report the identification of cell-surface glucose-regulated protein 78 kDa (GRP78) as a high-affinity receptor for ISM ($K_d = 8.6$ nM). We demonstrated that ISM-GRP78 interaction triggers apoptosis not only in activated ECs but also in cancer cells expressing high level of cell-surface GRP78. Normal cells and benign tumor cells tend to express low level of cell-surface GRP78 and are resistant to ISM-induced apoptosis. Upon binding to GRP78, ISM is internalized into ECs through clathrin-dependent endocytosis that is essential for its proapoptotic activity. Once inside the cell, ISM co-targets with GRP78 to mitochondria where it interacts with ADP/ATP carriers on the inner membrane and blocks ATP transport from mitochondria to cytosol, thereby causing apoptosis. Hence, ISM is a novel proapoptotic ligand that targets cell-surface GRP78 to trigger apoptosis by inducing mitochondrial dysfunction. The restricted and high-level expression of cell-surface GRP78 on cancer cells and cancer ECs make them uniquely susceptible to ISM-targeted apoptosis. Indeed, systemic delivery of recombinant ISM potently suppressed subcutaneous 4T1 breast carcinoma and B16 melanoma growth in mice by eliciting apoptosis selectively in the cancer cells and cancer ECs. Together, this work reveals a novel ISM-GRP78 apoptosis pathway and demonstrates the potential of ISM as a cancer-specific and dual-targeting anticancer agent.
Cell Death and Differentiation (2014) **21,** 797–810; doi:10.1038/cdd.2014.3; published online 24 January 2014

Angiogenesis is one of the limiting steps in tumor progression and metastasis.[1,2] Understanding the regulatory network of angiogenesis is important for developing effective treatment for cancer. Therefore, identification of novel angiogenic inhibitors and clarification of their downstream signaling hubs will provide new therapeutic strategies in antiangiogenic cancer therapy.

Isthmin (ISM) is a recently characterized endogenous inhibitor of angiogenesis.[3] It is a secreted 60-kDa protein, containing a centrally located thrombospondin type I repeat domain and a C-terminal adhesion-associated domain in MUC4 and other proteins (AMOP).[4] Recombinant ISM (rISM) potently induced endothelial cell (EC) apoptosis and suppressed angiogenesis *in vitro*. Stable overexpression of ISM in B16 melanoma cells strongly suppressed subcutaneous tumor growth in mice with accompanied reduction in tumor angiogenesis and increased cell death in tumors.[3] However, the molecular mechanism by which ISM mediates antiangiogenesis remains to be fully resolved. It is also not established whether ISM can function as an effective anticancer agent when delivered systemically.

Previously, we have identified the $\alpha v\beta 5$ integrin as a low-affinity EC surface receptor of ISM.[5] However, blocking $\alpha v\beta 5$ integrin only partially blocked the proapoptotic function of ISM. Hence, additional cell-surface receptor(s) may exist for mediating the proapoptotic function of ISM. Furthermore, under different physical conditions, ISM induced distinct responses from adherent ECs.[5] Although soluble ISM induces EC apoptosis, surface-immobilized ISM promotes EC adhesion and survival. How can a single ligand in different physical forms induce opposing cell responses remain to be resolved.

Glucose-regulated protein of 78 kDa (GRP78) is a member of the heat-shock chaperon family that mainly resides in ER and facilitates protein folding. It is a stress-response protein that is overexpressed in cells under stress. Cancer cells are under constant stress owing to their microenvironment of hypoxia, acidity and metabolic toxicity. A portion of the overexpressed GRP78 becomes translocated to cell surface. Although intracellular GRP78 is known for its pro-survival and anti-apoptotic function, cell-surface GRP78 serves as a receptor for proapoptotic ligands such as Kringle-5 (K5) and Par-4, thereby promoting apoptosis.[6,7] As cell-surface GRP78 is preferentially present in cancer cells, it is an attractive target for cancer therapy.[8–10] Indeed, synthetic peptides containing cell-surface GRP78-binding motifs conjugated to proapoptotic peptide suppressed primary tumor growth as well as established micrometastasis in mice.[11,12] Furthermore, a natural human IgM antibody targeting cell-surface GRP78, PAT-SM6, induces apoptosis in primary human multiple myeloma cells.[13]

[1]Department of Biological Sciences, National University of Singapore, Singapore, Singapore; [2]Department of Pharmacy, National University of Singapore, Singapore, Singapore; [3]Department of Obstetrics and Gynaecology, Yong Loo Lin School of Medicine, National University of Singapore, Singapore, Singapore and [4]Department of Molecular Pathology and Tumor Pathology, Akita University Graduate School of Medicine, Akita, Japan
*Corresponding author: R Ge, Department of Biological Sciences, National University of Singapore, Singapore 117543, Singapore. Tel: +65 65167879; Fax: +65 67792486; E-mail: dbsgerw@nus.edu.sg
Keywords: Isthmin; GRP78; apoptosis; cancer; angiogenesis; mitochondrial dysfunction
Abbreviations: ISM, Isthmin; GRP78, glucose-regulated protein of 78 kDa; AAC, ADP/ATP carrier
Received 22.6.13; revised 15.12.13; accepted 23.12.13; Edited by L Scorrano; published online 24.1.14

In this work, we report that ISM is a novel proapoptotic ligand for cell-surface GRP78. Upon binding GRP78, ISM is internalized through clathrin-dependent endocytosis and targets to mitochondria where it interacts with ADP/ATP carriers (AACs) and blocks ADP/ATP exchange, thereby resulting in cell death.

Results

Soluble ISM is internalized into ECs through clathrin-dependent endocytosis and internalization is critical for its proapoptotic/antiangiogenic function. To explore whether differences in ISM internalization into ECs via endocytosis could have a role in the opposing effects induced by soluble *versus* immobilized ISM, ECs were incubated with soluble rISM or seeded onto rISM pre-coated plate. After washing off the extracellular rISM, internalized rISM was examined by western blotting (WB). As shown in Figure 1a, only soluble rISM was internalized into ECs. This internalization was both dose- and time-dependent (Figures 1b and c). Within 5 min of rISM incubation with ECs, rISM was already detectable inside the cell.

In eukaryotic cells, the major endocytic pathways are clathrin-dependent and clathrin-independent/lipid-raft-mediated route.[14] To determine the route of ISM internalization, ECs were pretreated with chlorpromazine (inhibitor of clathrin-dependent endocytosis) or nystatin (inhibitor of lipid-raft-dependent endocytosis) at various concentrations before rISM incubation.[15,16] As shown in Figure 1d, chlorpromazine but not nystatin inhibited ISM internalization in a dose-dependent manner. Immunofluorescent (IF) staining revealed that only chlorpromazine could suppress rISM accumulation in the cytosol (Figure 1e). These results indicate that soluble ISM is internalized through clathrin-dependent endocytosis.

To study whether internalization is important for the proapoptotic/antiangiogenic function of ISM, chlorpromazine and nystatin were applied into EC tube formation and apoptosis assays together with ISM. Only chlorpromazine significantly interfered with ISM-mediated antiangiogenesis and apoptosis (Figures 1f and g). Chlorpromazine and nystatin together did not result in a bigger inhibiting effect on ISM's functions than chlorpromazine alone. Thus, ISM internalization into ECs via clathrin-dependent endocytosis is essential for its proapoptotic/antiangiogenic function.

Cell-surface GRP78 is a high-affinity receptor for ISM and mediates ISM's proapoptotic/antiangiogenic function. ISM binds to EC surface with a K_d in the nM range (data not shown). However, the only known cell-surface receptor for ISM, $\alpha v\beta 5$ integrin, binds ISM with a K_d in the μM range.[5] Hence, there exists unknown high-affinity receptor(s) of ISM that may have important roles in mediating its function. To search for this high-affinity receptor, we isolated EC plasma membrane protein fraction with and without prior incubation with rISM (His-tagged). After Ni-NTA beads pull down, the bound proteins were analyzed by SDS-PAGE. Specific bands in ISM-treated EC plasma membrane fraction were identified by mass spectrometry (MS) (Figure 2a, Supplementary Figures S1a and b). Potential ISM-interacting proteins were identified including clathrin heavy chain (CHC) and GRP78. As clathrin is the key protein mediating clathrin-dependent endocytosis,[17] association of CHC with ISM supports the results above that ISM is internalized through clathrin-dependent endocytosis (Figure 1).

GRP78 is traditionally regarded as a ER lumen chaperon protein for facilitating protein folding and mediate cellular stress response.[18,19] Recently, it has emerged that GRP78 is also present on the cell surface under stress.[20] Cell-surface GRP78 acts as an important regulator in tumor progression, metastasis, angiogenesis and resistance to cancer therapy.[9,10,21] To confirm the interaction between GRP78 and ISM, we performed co-immunoprecipitation (co-IP) experiment by incubating ISM with plasma membrane fraction of HUVECs. ISM interacted with GRP78 from EC plasma membrane fraction (Figure 2b). Binding affinity between recombinant GRP78 (rGRP78) and rISM is high with a $K_d = 8.58$ nM (Figure 2c). The number of cell-surface GRP78 molecules ($(3.28 \pm 0.57) \times 10^5$) is $\sim 8\times$ more than the number of $\alpha v\beta 5$ integrin ($(4.27 \pm 0.50) \times 10^4$) in each HUVEC. Thus, ISM binds to ECs predominantly through GRP78 because of greater abundance and higher binding affinity of this receptor.

To investigate whether cell-surface GRP78 mediates ISM's function, we first determined that GRP78 is important for EC attachment to ISM-coated surface. Anti-GRP78 antibody partially compromised EC adhesion to ISM-coated surface in similar fashion as anti-$\alpha v\beta 5$ integrin antibody (Figure 2d). Furthermore, anti-GRP78 antibody dose-dependently interrupted ISM's anti-tube formation and proapoptotic activity (Figures 2e and f). Knockdown of GRP78 expression in HUVECs by siRNAs also suppressed EC attachment to ISM-coated surface, as well as its antiangiogenic and proapoptotic activity (Supplementary Figure S2). These results demonstrated that GRP78 is a functional cell-surface high-affinity receptor of ISM.

GRP78 mediates ISM internalization. As internalization into ECs is critical for ISM's antiangiogenic and proapoptotic function, we investigated the role of cell-surface GRP78 in ISM internalization. Blocking cell-surface GRP78 by anti-GRP78 antibody dose-dependently reduced ISM internalization into HUVECs (Supplementary Figure S3a). Triton-partitioning experiment using ISM-treated HUVECs indicated that ISM and GRP78 are both present in non-lipid-raft fraction, sharing similar distribution with CHC (a marker for clathrin-dependent pathway) but not caveolin (a marker for clathrin-independent/lipid-raft-mediated pathway). In contrast, the other ISM receptor, $\alpha v\beta 5$ integrin, is distributed more with caveolin-positive lipid-raft fraction, distinct from ISM and GRP78 (Supplementary Figure S3b).

Transient overexpression of GRP78 but not $\alpha v\beta 5$ integrin in LS174T cells increased ISM internalization in a dose-dependent manner. Simultaneous overexpression of both GRP78 and $\alpha v\beta 5$ integrin promoted ISM internalization to the same extent as GRP78 overexpression alone, indicating that $\alpha v\beta 5$ integrin is not involved in ISM internalization (Supplementary Figure S3c).

Together, these results confirm that cell-surface GRP78 mediates ISM internalization.

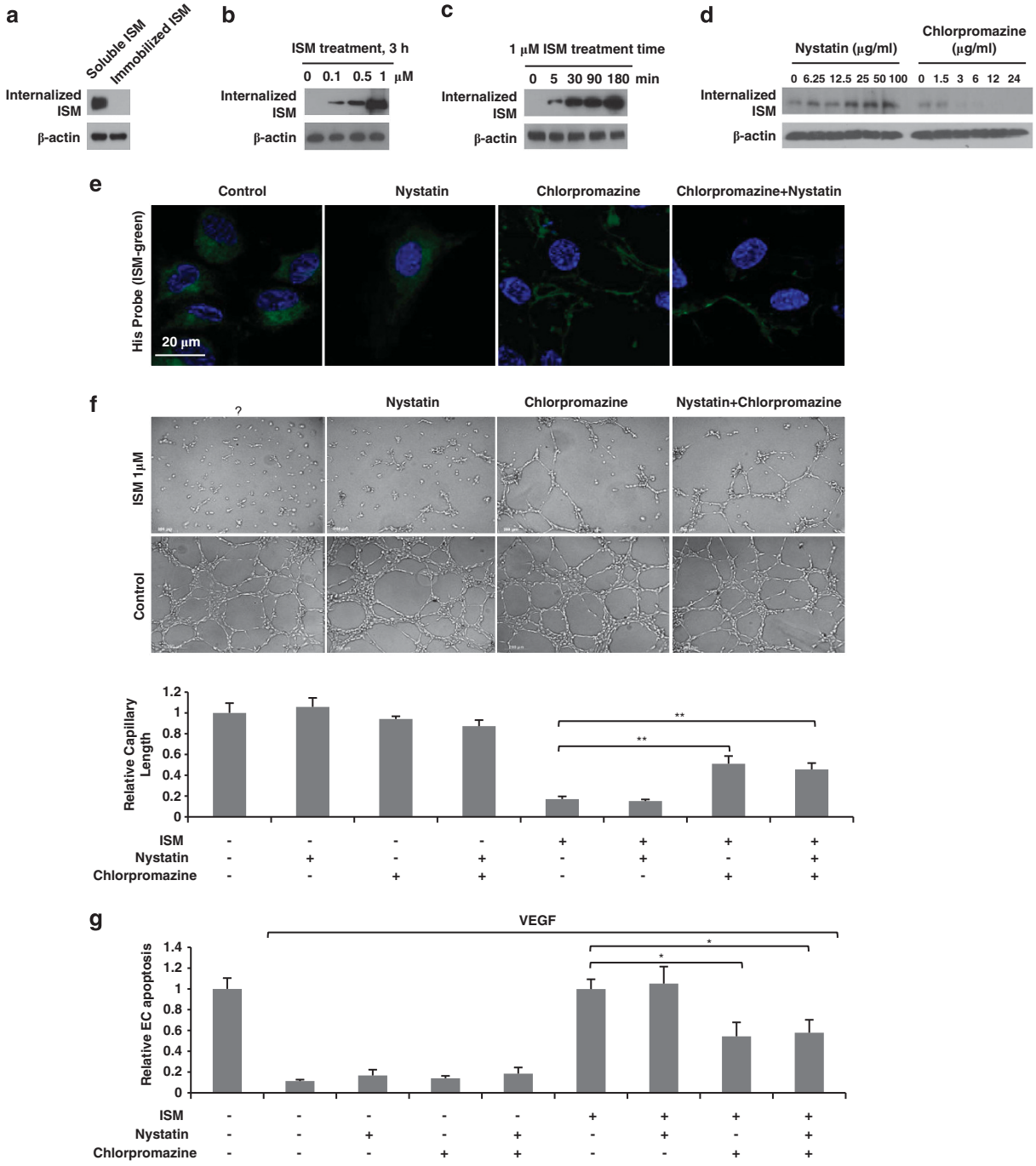

Figure 1 ISM is internalized into ECs through clathrin-dependent endocytosis and internalization is critical for its antiangiogenic/proapoptotic function. (**a**) Soluble but not immobilized ISM was internalized into ECs. (**b**) ISM was internalized into ECs in a dose-dependent manner. (**c**) ISM was internalized into ECs in a time-dependent manner. (**d**) Internalization of ISM was blocked by chlorpromazine but not nystatin in a dose-dependent manner. (**e**) IF detection of internalized ISM in control, nystatin or chlorpromazine pretreated HUVECs. ISM (green) internalization was only suppressed by chlorpromazine treatment. Nuclei were stained with DAPI (blue). (**f**) Chlorpromazine, but not nystatin, effectively reduced the anti-tube formation activity of ISM. $^{**}P<0.01$, $n=3$. Error bars denote S.E.M. (**g**) Chlorpromazine, but not nystatin, significantly impaired the proapoptotic activity of ISM on ECs. $^{*}P<0.05$, $n=3$. Error bars denote S.E.M.

ISM selectively induces apoptosis in cells that exhibit high-level cell-surface GRP78. As the first report of cell-surface GRP78 on malignant T lymphocytes in 1997, it is now well established that GRP78 exists on the cell surface of cancer cells and cancer ECs.[20,22] Overexpression of GRP78 triggers the re-localization of GRP78 to cell surface and is associated with advanced stages of tumor progression and invasiveness.[8,23] Thus, we investigated the relationship between levels of cell-surface GRP78 and susceptibility of cells to ISM-induced apoptosis.

HUVECs express a much higher cell-surface GRP78 than LS174T cells, a non-metastatic human colon carcinoma cell

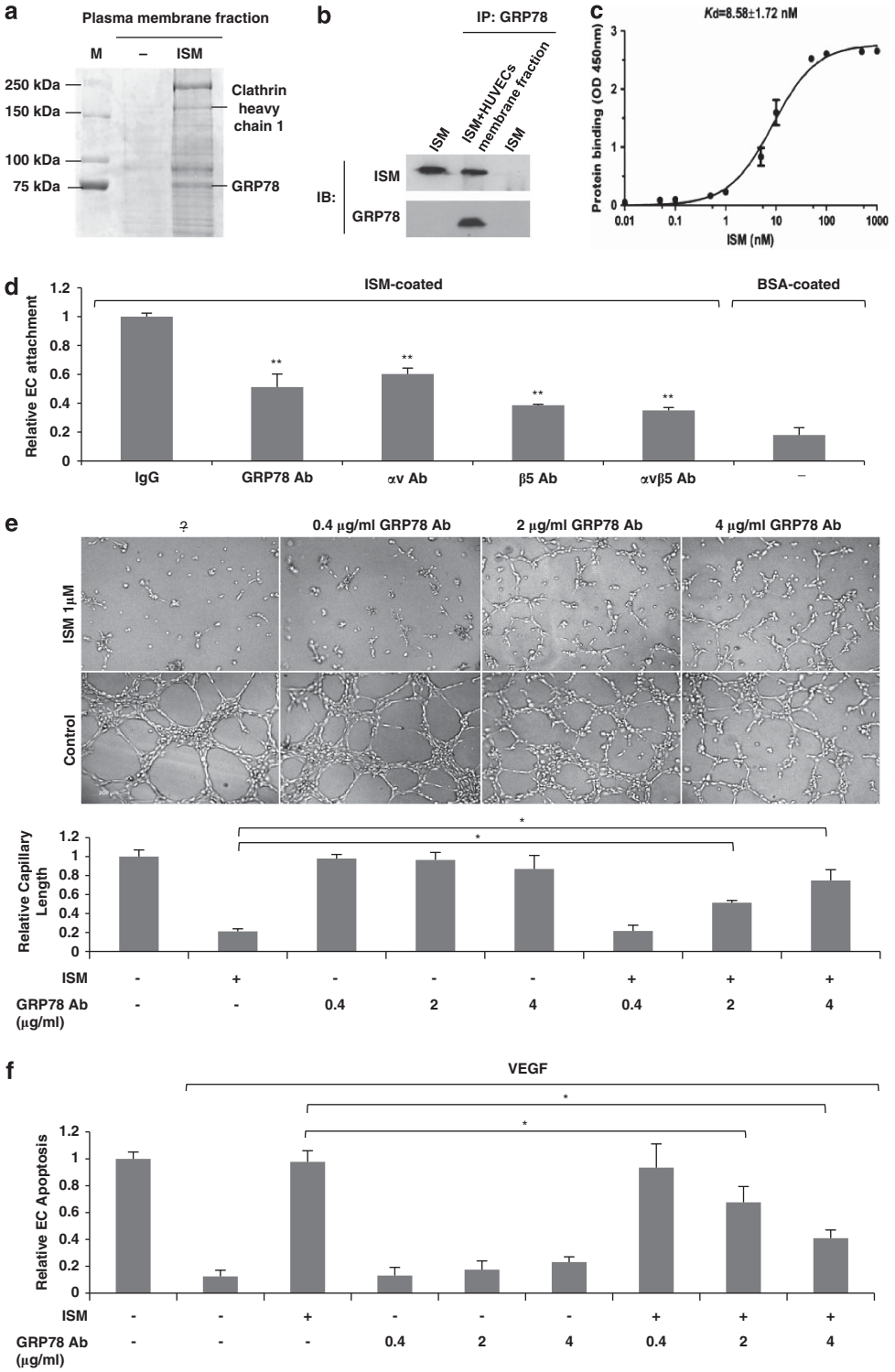

Figure 2 GRP78 is a high-affinity cell-surface receptor for ISM and it is required for mediating ISM-induced antiangiogenesis and apoptosis. (**a**) Identification of ISM's binding partners in plasma membrane. (**b**) ISM co-IP with GRP78 from HUVECs plasma membrane fraction. (**c**) Determination of binding affinity between ISM and GRP78; $n=3$. (**d**) Similar with $\alpha v\beta 5$ integrin antibodies, GRP78 antibody partially blocked ISM-mediated ECs adhesion. $^{**}P<0.01$, $n=3$. Error bars denote S.E.M. (**e**) Anti-GRP78 antibody interfered with the anti-tube formation action of ISM in a dose-dependent manner. $^{*}P<0.05$, $n=3$. Error bars denote S.E.M. (**f**) Anti-GRP78 antibody dose-dependently blocked ISM-induced EC apoptosis. $^{*}P<0.05$, $n=3$. Error bars denote S.E.M.

line (Figure 3a). Although HUVECs are highly susceptible to ISM-induced apoptosis, LS174T is relatively resistant (Figures 3b and c). When we artificially overexpressed GRP78 in LS174T cells by transient transfection, LS174T cells became susceptible to ISM-induced apoptosis in a GRP78 dose-dependent manner (Figure 3d). Thus, levels of cell-surface GRP78 correlate with the apoptotic effect of ISM.

Indeed, ISM only induced significant apoptosis in cells that express high-level cell-surface GRP78 including HUVECs, HEK293T (transformed human embryonic kidney cells), B16F10 (mouse melanoma), 4T1 (mouse breast cancer), 786-O (human renal carcinoma) and LS-LM6 (highly liver-metastatic human colon cancer) (Supplementary Figure S4). In contrast, no significant apoptosis is induced by ISM in cells that express a low level or no cell-surface GRP78 such as LS174T, NIH3T3 and SWISS3T3 (Supplementary Figure S4). Notably, LS-LM6, a highly metastatic derivative of LS174T, expresses high-level cell-surface GRP78 and is susceptible to ISM-induced apoptosis (Supplementary Figure S4).[24]

Overexpression of ISM's low-affinity receptor $\alpha v\beta 5$ integrin also increased the sensitivity of LS174T cells to ISM-induced apoptosis (Supplementary Figure S5a). ISM is known to interact with $\alpha v\beta 5$ integrin and trigger cell death through integrin-mediated activation of caspase-8.[5] Simultaneous GRP78 and $\alpha v\beta 5$ integrin overexpression led to more apoptosis than GRP78 or $\alpha v\beta 5$ integrin alone (Supplementary Figure S5b). Thus, ISM can induce apoptosis through both cell-surface GRP78 and $\alpha v\beta 5$ integrin.

ISM co-targets with cell-surface GRP78 to mitochondria. To decipher how ISM induces apoptosis through cell-surface GRP78, we investigated the localization of internalized ISM in the cell. Secretive ISM-GFP and GFP expression vectors were transiently transfected into HUVECs and HEK293T cells. Expressed ISM-GFP fusion protein was secreted into the culture media ($\sim$9.7 nM) and endocytosed back into cells through binding to cell-surface GRP78. Internalized ISM-GFP was co-localized in a clustered manner in cytosol and co-localize with mitochondria in both HUVECs and HEK293T cells (Figure 4a). In comparison, endocytosed secreted GFP was diffusely distributed in the whole cell (data not shown). The Pearson's correlation coefficient R_p between ISM-GFP and mitochondria is 0.822 in HUVECs and 0.941 in HEK293T, respectively, indicating that internalized ISM-GFP co-localizes with mitochondria. In comparison, R_p values between GFP and mitochondria were around 0 in both cell types (data not shown). Similarly, internalized rISM (1 μM) was co-localized with mitochondria in HUVECs with $R_p = 0.85$ (Figure 4b). As HUVECs tend to shrink upon 1 μM rISM treatment due to apoptosis, the mitochondrial network morphology also changes correspondingly (Figures 4a and b). This change is suppressed in the presence of the pan-caspase inhibitor Z-VAD-fmk (Supplementary Figure S6a). These data demonstrates that internalized ISM is targeted to mitochondria.

The mitochondria localization of internalized ISM was further confirmed by cell fractionation from HUVECs and HEK293T transfected with a secretive his-tagged ISM expression vector. The internalized ISM (detected by anti-his antibody to distinguish from endogenous ISM) is predominantly localized in mitochondria (Figure 4c). Similarly, incubation of rISM with cultured HUVECs also resulted in rISM being localized to mitochondria (Figure 4d).

To identify the mitochondria proteins that interact with ISM, we pulled down his-tagged ISM and its binding partners from the mitochondrial lysates from ISM-transfected HEK293T cells.

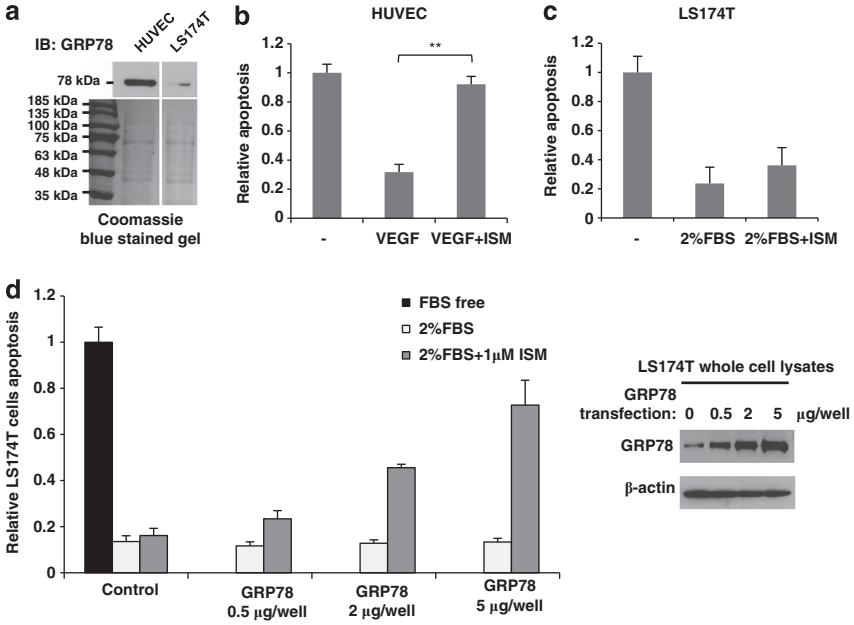

Figure 3 Cell-surface GRP78 sensitizes cells to ISM-induced apoptosis. (**a**) GRP78 levels in the plasma membrane fraction of HUVEC and LS174T cells. Equal amount of plasma membrane proteins were loaded as shown in the Coomassie blue-stained gel. (**b**) ISM-induced significant apoptosis in HUVECs. $^{**}P < 0.01$, $n = 3$. Error bars denote S.E.M. (**c**) LS174T cells were resistant to ISM-induced apoptosis. (**d**) Increasing GRP78 expression level by transient transfection progressively sensitized LS174T cells to ISM-induced apoptosis dose dependently

Proteins that interact with ISM were identified by SDS-PAGE and MS. Both CHC and GRP78 were identified, consistent with GRP78 being the receptor mediating ISM endocytosis through clathrin-dependent pathway (Figure 4e and Supplementary Figure S1). Hence, internalized ISM co-targets with cell-surface GRP78 to mitochondria. Indeed, WB revealed the co-presence of GRP78 and ISM in mitochondria of cells overexpressing exogenous ISM (Figure 4c). Similarly, upon rISM treatment of HUVECs, GRP78 also became translocated into mitochondria together with rISM (Figure 4d). These results revealed that ISM co-targets with GRP78 to mitochondria.

ISM blocks ATP transport from mitochondria to cytosol through interaction with AACs. AAC2 and AAC3 were identified as ISM-interacting proteins in mitochondria (Figure 4e). AAC, also known as adenine nucleotide translocase or ADP/ATP translocase, is the major ADP/ATP transporter located on the mitochondria inner membrane, catalyzing the exchange of ATP produced in mitochondria matrix with ADP in cytosol.[25] Four AAC isoforms have been identified in human with distinct expression patterns.[26,27] According to previous reports,[28–30] AAC2 and AAC3 are the dominant AACs in ECs. Co-IP confirmed that ISM interacts with AAC2/AAC3 (Figure 5a). Furthermore, internalized ISM-GFP co-localized with mCherry-AAC2 (Supplementary Figure S6b). Hence, internalized ISM is targeted to mitochondria where it interacts with AACs on the mitochondria inner membrane.

By binding to AAC2/AAC3, ISM could interfere with ADP/ATP exchange. Indeed, cytosolic ATP level was reduced to $>50\%$ upon ISM treatment (Figure 5b). On the other hand, mitochondrial ATP level was increased $\sim 40\%$ (Figure 5c). These data suggest that ISM blocked the exchange of cytosolic ADP against mitochondria matrix ATP across the mitochondrial inner membrane. In addition, ATP level in the whole-cell lysates was also decreased around 50% after ISM treatment (Figure 5d). This is not surprising as AACs catalyze the 1 : 1 exchange of ADP against ATP. Blockage of AAC function would result in ADP (the material for ATP synthesis) shortage in mitochondrial matrix, leading to reduction of ATP generation. Indeed, levels of ADP were affected in the opposite direction of ATP in various locations (Supplementary Figures S6c–e). Interestingly, suppression of ADP/ATP exchange by ISM was unaffected by presence of the pan-caspase inhibitor Z-VAD-fmk (Figures 5b–d; Supplementary Figure S6c–e). Therefore, the reduction of cytosolic ATP level upon ISM treatment is independent of caspase-8 activation triggered by ISM-αvβ5 integrin interaction. Cytosolic ATP reduction is likely the cause rather than consequence of ISM-triggered apoptosis. ATP is critical for cell survival and depletion of cellular ATP of 25–70% cause apoptosis.[31] Partial ATP depletion has been reported to result in caspase-8 and caspase-3 activation in MDCK cells.[32] Hence, ISM induces apoptosis through GRP78-mediated mitochondria targeting and interference of ADP/ATP exchange between mitochondria and cytosol (illustrated in Figure 5g).

We further analyzed other aspects of mitochondrial perturbations. ISM did not affect mitochondrial membrane potential. After 24 h rISM treatment, when the nuclei of HUVECs were already condensed, which is a hallmark of apoptosis, mitochondria membrane potential remained unchanged as the marker dye for mitochondrial membrane potential TMRM remained positively stained (Figure 5e). Similarly, the release of proapoptotic factors such as cytochrome *c* and AIF from mitochondria to cytoplasm was also not observed (Figure 5f). Therefore, ISM induced mitochondrial dysfunction and apoptosis without inducing the intrinsic apoptotic pathway.[33]

GRP78 and αvβ5 integrin function as independent cell-surface receptors for ISM and mediate EC apoptosis through distinct signaling pathways. Both GRP78 and αvβ5 integrin serve as cell-surface receptor for ISM and mediate its antiangiogenic/proapoptotic function. However, whether these two receptors function cooperatively or independently remain unknown. Using proximity ligation assay (PLA), a method allowing visualization and quantification of specific protein interaction events *in situ*, we determined whether GRP78 directly interacts with αvβ5 integrin in HUVECs. PLA signal represents direct interaction between two proteins in their native state and location.[34] No interaction between GRP78 and αvβ5 integrin were detected in the presence or absence of ISM (Figures 6a and b). In contrast, positive PLA signals were evident between ISM and its two receptors. Notably, the PLA signal between ISM and GRP78 was 12-fold higher than that between ISM and αvβ5 integrin. This reflected the 8 times more cell-surface GRP78 molecules on each HUVEC plus the 100 times higher binding affinity between ISM and GRP78.[5] Co-IP using both EC plasma membrane fraction or recombinant GRP78 and αvβ5 integrin heterodimer further confirmed that there was no interaction between GRP78 and αvβ5 integrin (Figures 6c and d).

GRP78 and αvβ5 integrin also presented distinct distribution patterns without any significant co-localization in tumors after systemic ISM treatment (Supplementary Figure S7). Intravenously delivered rISM internalized into cancer cells and co-localized with GRP78 but not αvβ5 integrin in both B16 and

Figure 4 GRP78 mediates ISM internalization and co-targets with ISM to mitochondria. (**a**) IF showing internalized ISM-GFP co-localized with mitochondria in HUVECs (top panel) and HEK293T cells (bottom panel) transfected with vector coding for ISM-GFP. The medium GRP78-GFP concentration in HUVECs 48 h post transfection is ~ 9.7 nM (data not shown). (**b**) IF showing internalized rISM (his-tagged) co-localized with mitochondria in HUVECs. rISM (1 μM) was added to HUVECs for 24 h before processed for IF. Quantitative measurements of Pearson's correlation coefficient (R_p) between red and green fluorescent labeled channels are indicated in the rightmost panel of each row. (**c**) ISM from transient transfection was mainly existed in mitochondria of HEK293T cells and HUVECs. GRP78 is co-localized into mitochondria with ISM in ISM-overexpressing HUVECs and HEK293T cells. VDAC was used as the marker for mitochondria; integrin β3 was used as the marker for plasma membrane; PDI was used as the marker for ER; β-actin was used as the marker for cytoplasm. WL, whole-cell lysates; Mito, mitochondrial fraction; PM, plasma membrane fraction; ER, endoplasmic reticulum fraction; C, cytoplasmic fraction. (**d**) Intracellular rISM resulted from incubation of HUVECs with rISM was mainly detected in mitochondria. GRP78 was co-localized to mitochondria with extracellular rISM in HUVECs. (**e**) ISM's-binding partners in mitochondrial lysates

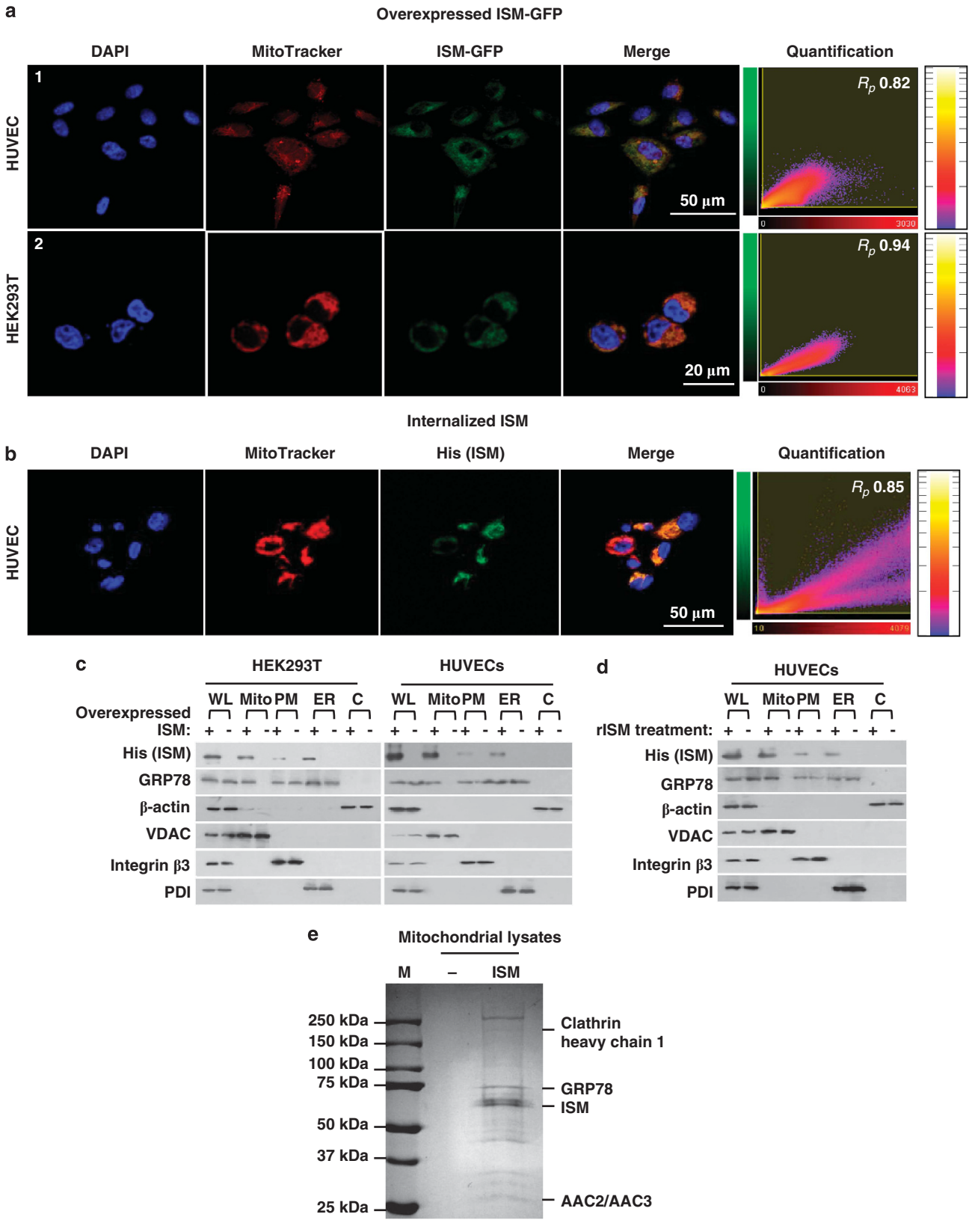
a
Overexpressed ISM-GFP
DAPI
MitoTracker
ISM-GFP
Merge
Quantification
HUVEC
HEK293T
1
2
50 μm
20 μm
R_p 0.82
R_p 0.94
Internalized ISM
b
DAPI
MitoTracker
His (ISM)
Merge
Quantification
HUVEC
50 μm
R_p 0.85
c
HEK293T
HUVECs
WL
Mito
PM
ER
C
Overexpressed ISM:
His (ISM)
GRP78
β-actin
VDAC
Integrin β3
PDI
d
HUVECs
rISM treatment:
e
Mitochondrial lysates
M
–
ISM
250 kDa
150 kDa
100 kDa
75 kDa
50 kDa
37 kDa
25 kDa
Clathrin heavy chain 1
GRP78
ISM
AAC2/AAC3

4T1 tumors (Figures 6e and f, and data not shown). Hence, GRP78 and $\alpha v\beta 5$ integrin function as independent receptors for ISM with GRP78 being the main mediator of ISM-induced apoptosis.

Systemically delivered rISM suppresses tumor growth in mice by inducing apoptosis of both cancer cells and cancer ECs. As GRP78 is highly expressed in cancer cells and cancer ECs in B16 melanoma and 4T1 breast carcinoma,

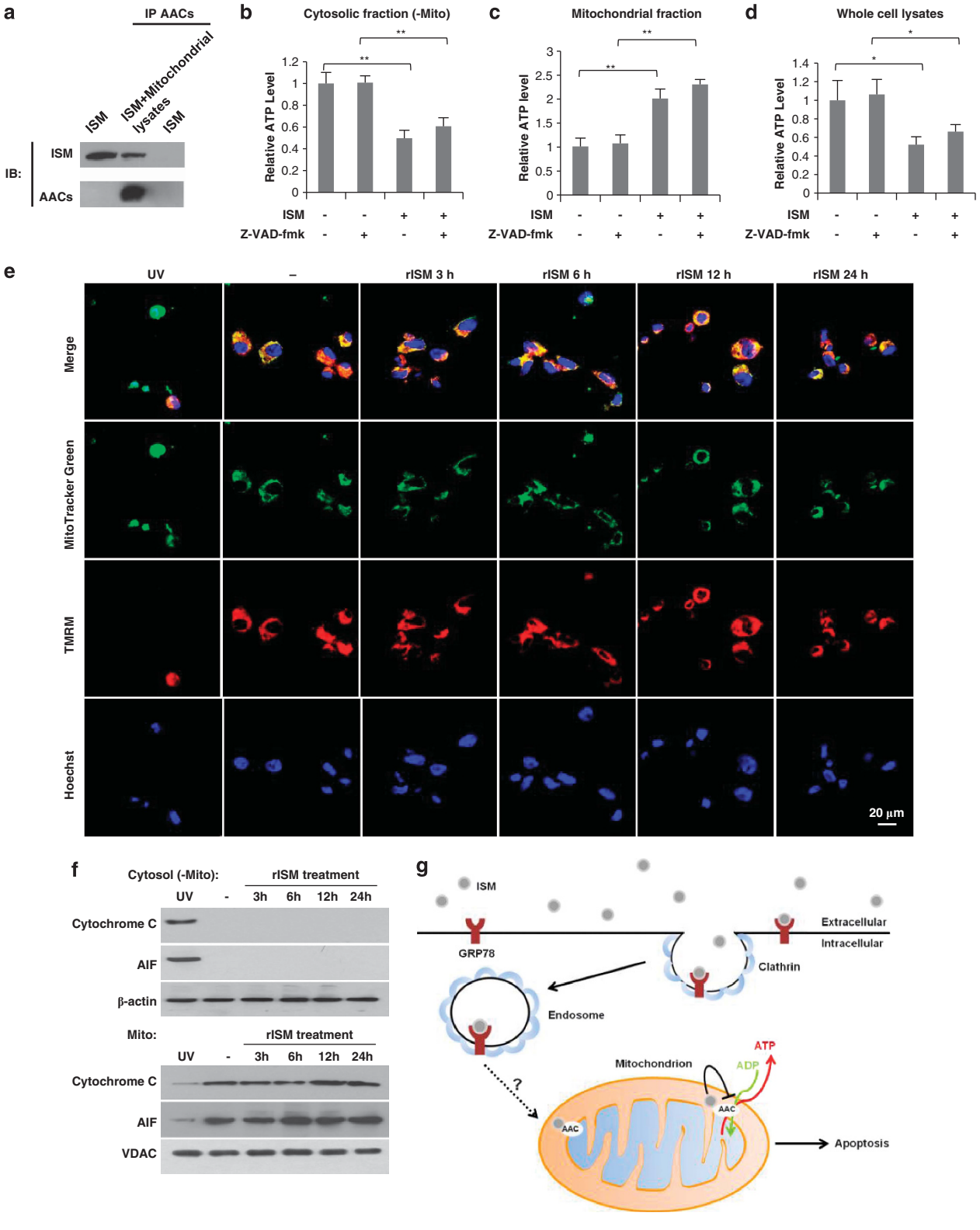

we next evaluated whether systemically delivered rISM can suppress tumor growth by targeting both types of cells in tumor (Figure 7). Intravenously delivered rISM potently suppressed 4T1 breast carcinoma and B16 melanoma growth in mice (Figures 8a–c; Supplementary Figure S8a–c). In addition, a marked decrease in blood vessels surrounding tumors in ISM-treated mice was also observed (Figure 8d; Supplementary Figure S8d).

In ISM-treated tumors, a significant reduction in tumor vascularization and cell proliferation accompanied with a substantial increase in apoptosis were observed (Figures 8e and f; Supplementary Figures S8e and f). Double staining of ECs (CD31) and apoptotic cells (TUNEL) indicated that ISM treatment induced apoptosis of both cancer cells and cancer ECs (Figure 8g; Supplementary Figure S8g). Increased cell death, reduced angiogenesis coupled with decreased cell proliferation is likely the reasons that contribute to reduced tumor growth in ISM-treated mice.

Discussion

The ER stress-response protein GRP78 has recently emerged as a promising target for anticancer therapeutics because of its restricted presence on the cell surface of cancer cells (invasive/metastatic cancers) and proliferating ECs but not in normal cells.[9,10,20] We report here that ISM is a novel extracellular ligand of cell-surface GRP78 and ISM-GRP78 interaction triggers apoptosis in both cancer cells and cancer ECs. ISM is thus a tumor-specific and dual-targeting anticancer protein.

We demonstrated that cell-surface GRP78 binds ISM with high affinity and mediates ISM internalization through clathrin-dependent endocytosis (Figures 1–3). Significantly, levels of cell-surface GRP78 correlate with the susceptibility of cells to ISM-induced apoptosis (Figure 3 and Supplementary Figure S4). Although the highly metastatic LS-LM6 express a high-level cell-surface GRP78 and is sensitive to ISM-induced apoptosis, its non-metastatic parental line LS174T is resistant, correlating with its low-level cell-surface GRP78 (Figure 3 and Supplementary Figure S4). It is noted that LS-LM6 cells also express a higher level of $\alpha v\beta 5$ integrin, the low-affinity receptor of ISM.[24] ISM-$\alpha v\beta 5$ integrin interaction may also contribute to its high sensitivity to ISM-induced apoptosis.

Cell-surface GRP78 is a receptor for several extracellular ligands including Par-4, plasminogen K5 and activated $\alpha 2$-macroglobulin ($\alpha 2M^*$). Although Par-4 and K5 both trigger apoptosis through GRP78, $\alpha 2M^*$-GRP78 interaction leads to enhancement of cell survival and proliferation.[20] Similar to ISM, K5 also induced apoptosis in both ECs and cancer cells that present a high-level cell-surface GRP78. However, while K5 only induced significant apoptosis in cultured B16F10 melanoma cells under hypoxia, ISM induced B16F10 apoptosis under normaxia (Supplementary Figure S4; Davidson *et al*.[6]). Par-4 induces apoptosis both intracellularly and extracellularly. Extracellular Par-4 binds to cell-surface GRP78 and induces apoptosis via TRAIL.[7]

Although K5 was hypothesized to be internalized into ECs, no experimental evidence has been presented.[6] We demonstrated here that ISM is efficiently internalized into ECs through clathrin-dependent endocytosis and internalization is essential for its antiangiogenic and proapoptotic function (Figure 1). The endocytosed ISM-GRP78 complex is targeted to mitochondria where ISM interacts with AACs on the inner membrane and blocks ADP/ATP exchange (Figures 4 and 5; Supplementary Figure S6). Reduction of cytosolic ATP may be the main mechanism of ISM-GRP78 induced apoptosis.

How ISM-GRP78 is targeted to mitochondria is not yet clear. Both ISM and GRP78 have no identifiable mitochondrial targeting sequence (predicted by MITOPROT: http://ihg.gsf.de/ihg/mitoprot.html). Co-IP experiment revealed no evidence that ISM binds to TOM20, the first receptor involved in recognizing the targeting sequence of a mitochondria protein in TOM complex that is known to mediate the import of mitochondria proteins through the outer membrane (data not shown).[35,36] In addition, no member of TOM complex was identified as binding partners for ISM in mitochondria (Figure 4e). Therefore, ISM is unlikely to be imported into mitochondria through TOM complex. Future work is needed to fully elucidate the mitochondria targeting mechanism of ISM-GRP78 and how it is regulated.

Several extracellular antiangiogenic proteins are known to be endocytosed into ECs and internalization is important for their antiangiogenic functions. For example, endostatin is endocytosed through both clathrin-dependent and caveaolae/lipid-raft-dependent pathways.[16] Enhancement of endostatin uptake into ECs increased its antiangiogenic activity. However, it is not clear where the internalized endostatin is targeted to inside the cell. On the other hand, angiostatin is internalized into ECs and targeted to mitochondria where it interacts with ATP synthase and malate dehydrogenase-2, thereby suppressing ATP production to induce apoptosis.[37]

We demonstrated here that internalization is the mechanism underling the distinct biological effect of soluble ISM on ECs. We envision that similar mechanism may also be responsible for mediating distinct functions associated with the soluble form of other extracellular antiangiogenic proteins. Both endostatin and thrombospondin-1 present proapoptotic activity when present in soluble form, but support EC adhesion and survival when immobilized.[38–40]

Figure 5 ISM interacts with AACs in mitochondria and blocks ATP transport from mitochondria to cytosol. (**a**) rISM co-IP with AACs in mitochondrial fraction of HUVECs. (**b**) rISM treatment reduced ATP level in cytosolic fraction of HUVECs independent of caspases activity. Z-VAD-fmk was used as pan-caspase inhibitor. $^{**}P<0.01$, $n=3$. Error bars denote S.E.M. (**c**) rISM treatment increased ATP level in mitochondrial fraction of HUVECs independent of caspases activity. Z-VAD-fmk was used as pan-caspase inhibitor. $^{**}P<0.01$, $n=3$. Error bars denote S.E.M. (**d**) rISM treatment diminished ATP concentration in whole-cell lysates of HUVECs independent of caspases activity. Z-VAD-fmk was used as pan-caspase inhibitor. $^{*}P<0.05$, $n=3$. Error bars denote S.E.M. (**e**) rISM treatment did not affect the mitochondrial potential of HUVECs. The UV-treated HUVECs were used as the positive control for the loss of mitochondrial potential via the intrinsic apoptotic pathway. The untreated HUVECs were used as the negative control. MitoTracker Green can stain mitochondria regardless of mitochondrial potential. TMRM (red) was used as the marker of mitochondrial potential. Nuclei were labeled by Hoechst (blue). (**f**) rISM treatment did not induce the release of cytochrome *c* and AIF from mitochondria to cytoplasm. The upper panel is the cytosolic fraction without mitochondria of HUVECs. The lower panel is the mitochondrial fraction. The UV-treated HUVECs were used as the positive control for the release of cytochrome *c* and AIF from mitochondria to cytoplasm via the intrinsic apoptotic pathway. β-actin was used as the marker for cytosolic fraction. VDAC was used the marker for mitochondria. (**g**) Schematic summary of the putative proapoptotic pathway engaged by ISM-GRP78 interaction

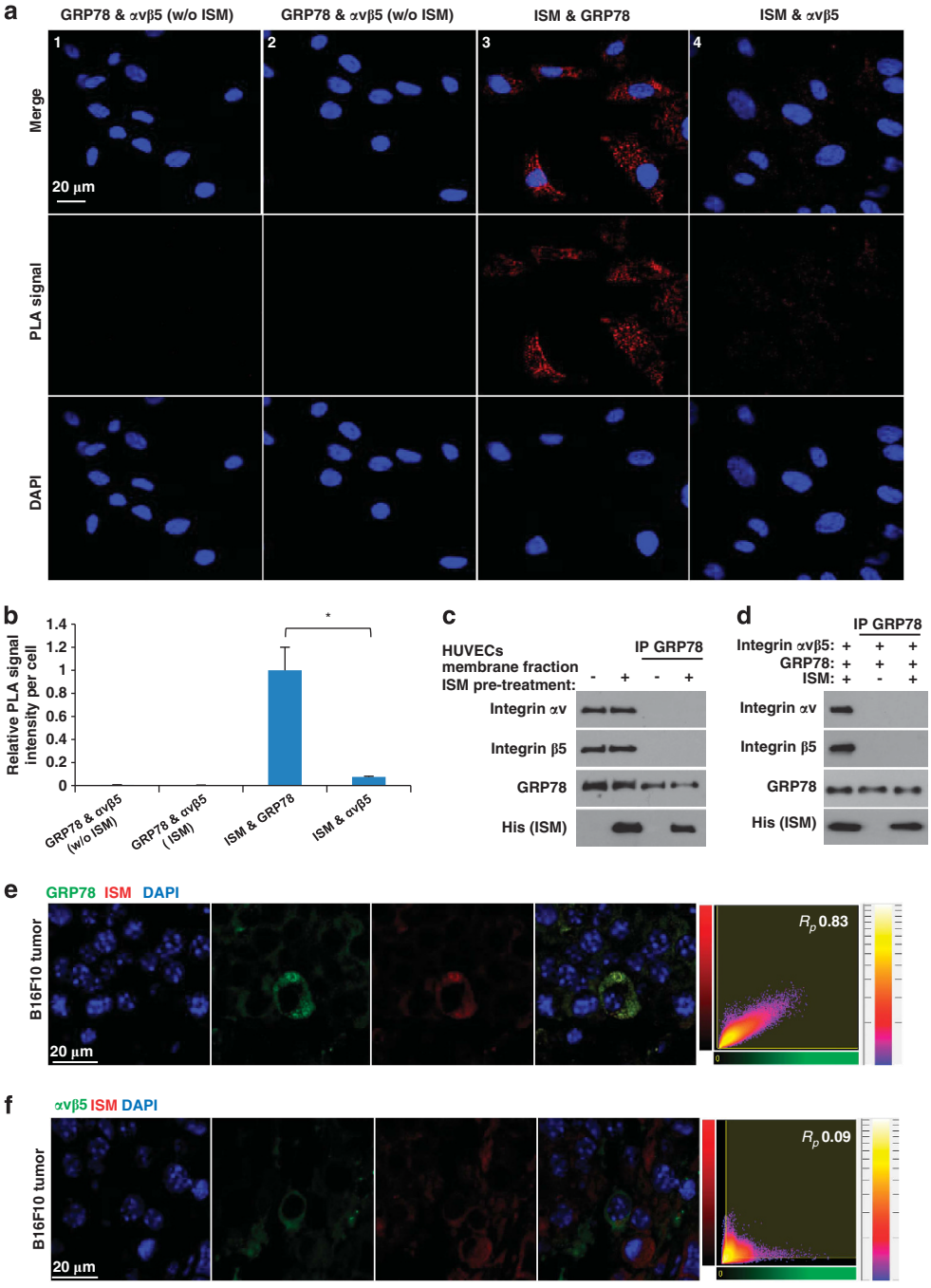

Figure 6 GRP78 and $\alpha v\beta 5$ integrin function as independent cell-surface receptor for ISM on ECs and mediating apoptosis through distinct signaling pathways. (**a** and **b**) GRP78 and $\alpha v\beta 5$ integrin do not interact in HUVECs. (**a**) Determination of the interaction between GRP78 and $\alpha v\beta 5$ integrin, ISM and GRP78, and ISM and integrin $\alpha v\beta 5$ by Duolink *in situ* PLA. PLA signals (red) indicate two proteins in close proximity (nucleus). GRP78 and $\alpha v\beta 5$ integrin did not exist in close proximity in HUVECs in the absence (1) or presence (2) of ISM; (3) ISM interacts with GRP78 on the cell surface and in the cytoplasm. (4) ISM interacts with $\alpha v\beta 5$ integrin in HUVECs. (**b**) Quantification of PLA signals. PLA signal intensities of three microscopic fields from each group were calculated by ImageJ and then normalized by cell number. All photos were obtained under the same exposure time and laser power. $^*P < 0.05$, $n = 3$. Error bars denote S.E.M. (**c**) GRP78 and $\alpha v\beta 5$ integrin did not bind to each other on the surface of HUVECs with or without ISM pretreatment. (**d**) Recombinant GRP78 and $\alpha v\beta 5$ integrin do not bind to each other with or without the presence of ISM. (**e** and **f**) Systemically delivered rISM is co-localized with GRP78, but not with $\alpha v\beta 5$ integrin, in B16F10 tumor cells. Paraffin sections of rISM-treated B16F10 tumors were probed for both GRP78 and ISM through IF using anti-his (red) and anti-GRP78 or $\alpha v\beta 5$ integrin (green) double staining. Nuclei were counterstained by DAPI (blue). Representative photos are shown. Quantitative measurements of the Pearson's correlation coefficient (*R*p) between red and green fluorescent labeled channels were indicated in the far-right

In summary, we report a novel ISM-GRP78 ligand-receptor signaling pathway that triggers apoptosis specifically in cancer cells and cancer ECs by inducing mitochondrial dysfunction. ISM thus bears tremendous potential as a cancer-specific and dual-targeting anticancer agent.

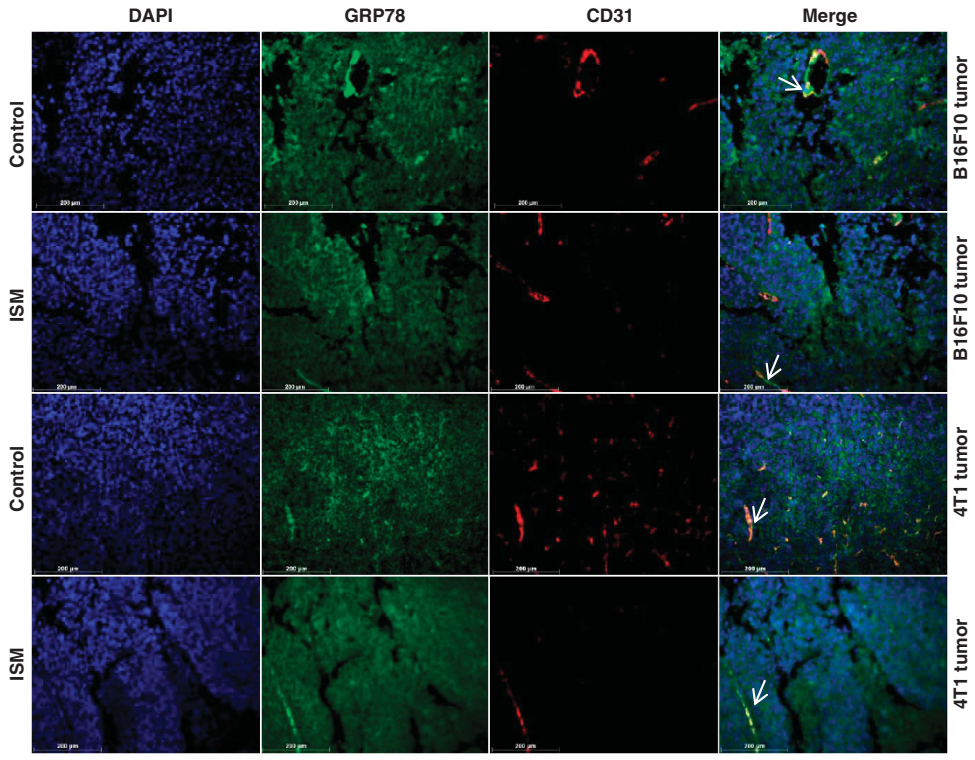

Figure 7 GRP78 is expressed in both cancer cells and cancer ECs. Expression of GRP78 in B16 melanoma and 4T1 breast carcinoma was probed by IF with anti-GRP78 (green) and double stained with anti-CD31 (red). Nuclei were counterstained by DAPI (blue). Co-localization of GRP78 and CD31 in ECs are indicated by white arrows

Materials and Methods

Cell lines, constructs and reagents. HUVECs were isolated and cultured as described.[41] LS174T and LS-LM6 cells were cultured as described.[24] HEK293T, B16F10, 4T1, 786-O, NIH3T3 and SWISS3T3 cells were purchased from ATCC (Manassas, VA, USA) and cultured in DMEM with 10% FBS (Sigma-Aldrich, St. Louis, MO, USA). GFP and mouse ISM cDNA were cloned into pSecTag2B vector (Invitrogen, Carlsbad, CA, USA). Human GRP78, integrin subunits-αv and -β5 cDNA were cloned into pXJ40 vector. Antibodies against integrin $\alpha v\beta 5$ (MAB1961Z; Millipore, Billerica, MA, USA), αv (MAB1980; Millipore), β5 (E-19; Santa Cruz Biotechnology, Santa Cruz, CA, USA), GRP78 (A-10, Santa Cruz Biotechnology) were used for neutralization. Other antibodies for WB, IF, co-IP, immunohistochemistry were mainly from Santa Cruz Biotechnology: CD31(M-20), PCNA (PC10), His-probe (H-15), β-actin (C4), VDAC (D16), GRP78 (E-4), AACs (N-19), integrin $\alpha v\beta 5$ (P1F76), αv (P2W7), β5 (H-96), β3 (PM6/13), PDI (A-1). Cytochrome *c* (556433) antibody was obtained from BD Pharmingen (San Jose, CA, USA). AIF (16501) antibody was obtained from Chemicon (Billerica, MA, USA). Secondary antibodies, DAPI and MitoTracker were from Invitrogen. TUNEL staining used an *in situ* cell death detection kit (Roche, Roche Diagnostics Asia Pacific, Singapore). Recombinant his-tagged ISM protein (rISM) and anti-ISM antibody were generated as described.[3]

Syngeneic tumorigenesis assay. 4T1 cells (1×10^6) were injected subcutaneously into the dorsal flank of 8-week-old female BALB/C mice. Two groups of mice ($n = 10$/group) received either PBS or 250 μg rISM through tail vein every other day from day 0 (date of inoculation) to day 22. Tumors were measured and processed for immunohistochemistry as described.[41]

Internalization assays. HUVECs 48 h post plasmid transfection or 30 min of nystatin and chlorpromazine (Sigma-Aldrich) treatment were incubated with 1 μM rISM for various time or different doses of rISM for 3 h. Cells were then incubated with MitoTracker for 30 min and washed by acidic PBS (pH 3.5) to remove surface bound rISM. Internalized rISM was detected by WB or IF staining using anti-his antibody. Images were collected by Zeiss LSM-510Meta confocal microscope (Carl Zeiss South East Asia, Singapore). The co-localization was analyzed by Imaris (Bitplane Inc., South Windsor, CT, USA). R_p ranges between 1 and -1. Value of 1 represents perfect correlation, 0 means no correlation.[42,43] It has been reported that R_p around 0.91 indicates that two images are almost identical,[44] and R_p around 0.75 shows a relatively high degree of co-localization.[45]

Tube formation assay. HUVECs were pretreated with 25 μg/ml nystatin, 6 μg/ml chlorpromazine or anti-GRP78 antibody for 15 min. Tube formation assay was performed in a μ-Slide Angiogenesis chamber (Ibidi, Martinsried, Germany) using *in vitro* angiogenesis assay kit (Millipore) as described.[41]

Apoptosis assay. HUVECs were pretreated with 25 μg/ml nystatin, 6 μg/ml chlorpromazine or anti-GRP78 antibody for 30 min after pre-starved in 2% FBS medium for 3 h. They were then treated with 1 μM rISM $+$ 15 ng/ml VEGF for 24 h. Non-EC cells were starved in serum-free medium for 6 h before been treated with 1 μM rISM in 2% FBS medium for 24 h. Apoptosis was determined by a DNA fragmentation cell death ELISA kit (Roche).

Cell attachment assay. HUVECs were pretreated by 4 μg/ml antibodies against integrin $\alpha v\beta 5$ and its individual subunit, GRP78 or control IgG for 30 min and the attachment assay was performed as described.[5]

Identify the cell-surface receptor of ISM. The plasma membrane fractions were isolated as described.[46] Ni-NTA beads (Promega, Madison, WI, USA) coupled with rISM were incubated with the plasma membrane fraction of HUVECs. Native beads were used as the control. Eluants were separated by SDS-PAGE. Specific bands were analyzed by MALDI-TOF-TOF MS (AB SCIEX, Framingham, MA, USA). The results were searched against NCBInr 080723 database.

Cell fractionation and identification of ISM-binding partners in mitochondria. Mitochondrial and cytosolic (without mitochondria) fractions of HUVECs or HEK293T cells either 48 h post pSecTag-ISM transfection or 24 h post 1 μM rISM treatment were isolated using the Mitochondria Isolation Kit (Thermo Scientific, Rockford, IL, USA). The rough ER microsomes were isolated as

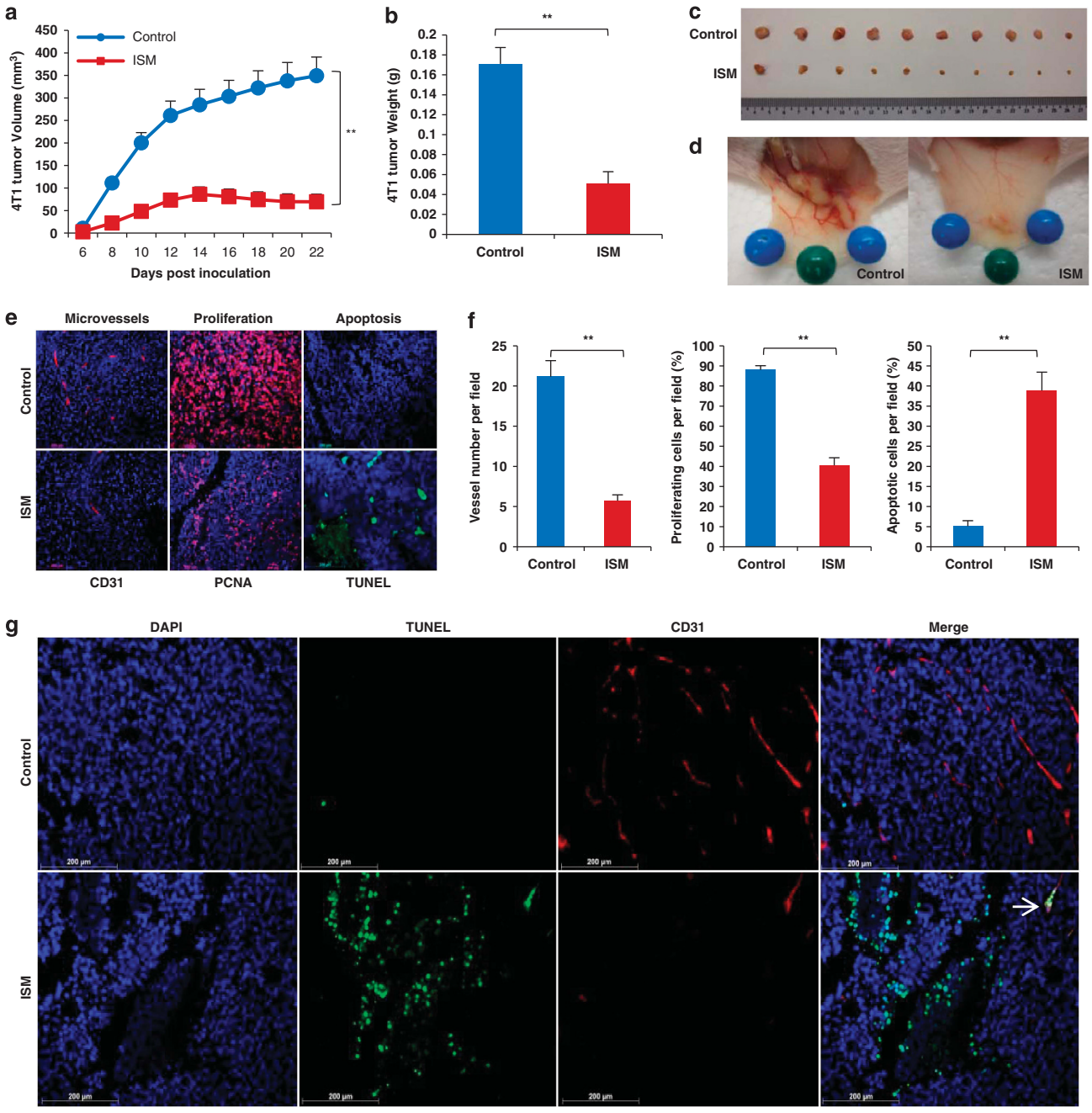

Figure 8 Systemically delivered rISM suppresses 4T1 breast carcinoma growth in mice by inducing apoptosis of both cancer cells and cancer ECs. (**a**–**d**) ISM inhibits 4T1 breast carcinoma growth in mice when delivered systematically. (**a**) 4T1 tumor growth curve in mice. *X*-axis represents the days after inoculation of 1×10^6 tumor cells. Groups consisted of control mice receiving no treatment or 250 μg rISM through tail vein injection every other day from day 0 (date of inoculation) to 22. $N = 10$. (**b**) Tumor weight at the end of the experiment (day 22). (**c**) Dissected tumors at the end of experiment. (**d**) rISM-treated tumors showed a reduced vascularization compared with untreated control. (**e**) rISM-suppressed tumor angiogenesis, proliferation and induced apoptosis in 4T1 tumor. Paraffin sections of 4T1 tumors from control and treated groups with rISM were probed for microvascular density (MVD), tumor cell proliferation and apoptosis through IF using anti-CD31, anti-PCNA and TUNEL staining, respectively. (**f**) Quantification of MVD, cell proliferation and apoptosis. Plots represent the mean of three fields per section, three sections per tumor and two tumors per group. $^{**}P < 0.01$. Error bars denote S.E.M. (**g**) ISM induces apoptosis of both cancer cells and cancer ECs in 4T1 breast carcinoma. Double IF using anti-CD31 (red) and TUNEL (green) is shown. Nuclei were counterstained by DAPI (blue). Representative photos are shown. Apoptotic EC is indicated by white arrow

described.[47,48] The mitochondrial fractions of pSecTag-ISM-transfected HEK293T cells and control cells were pulled down by μMACS anti-his microbeads (Miltenyi Biotec, Bergisch Gladbach, Germany). Eluants were separated by SDS-PAGE. Specific bands were analyzed by MALDI-TOF-TOF MS. The results were searched against NCBInr 080723 database.

ELISA-binding assay. Recombinant GRP78 (StressMarq Biosciences Inc., Victoria, BC, Canada) was pre-coated onto 96-well plate and saturation binding with increasing concentrations of rISM were carried out.[49] K_d was calculated using GraphPad Prism (GraphPad Software Inc., La Jolla, CA, USA).

Quantification of cell-surface GRP78 and integrin αvβ5 molecule numbers. Recombinant GRP78 or integrin αvβ5 (Millipore) were used to establish a standard curve using respective antibodies through ELISA. HUVEC plasma membrane fractions were analyzed similarly. The number of GRP78 or integrin αvβ5 receptors on each HUVEC was determined according to the protein standard. $^{*}P<0.05$, $n=4$.

Co-immunoprecipitation. Protein A/G agarose beads pre-bound with anti-GRP78 or anti-AAC antibody were incubated with rISM together with plasma membrane or mitochondrial lysate, respectively. Anti-GRP78 or anti-AAC antibody pre-bound agarose beads incubated with rISM only were used as the control. Eluants were analyzed by WB.

ATP colorimetric assay. The ATP concentrations in whole-cell lysate, mitochondrial and cytosolic (without mitochondria) fractions in HUVECs with indicated treatment of 1 μM rISM or 10 μM pan-caspase inhibitor, Z-VAD-fmk (Millipore), for 3 h were analyzed using the ATP colorimetric assay kit (BioVision, Milpitas, CA, USA).

Determination of mitochondrial potential. HUVECs were starved for 3 h in 2% FBS media and then incubated with 2% FBS medium containing 15 ng/ml VEGF and 1 μM rISM for indicated period of time. The HUVECs exposed to UV radiation for 30 min were used as the positive control for the loss of mitochondrial potential triggered by intrinsic apoptotic pathway. The untreated HUVECs were used as the negative control for the loss of mitochondrial potential. Then cells were treated by serum-free media containing 200 nM MitoTracker Green (M7514, Invitrogen), 600 nM TMRM (T668, Invitrogen) and 5 μg/ml Hoechst (H3570, Invitrogen) for 30 min before imaging. MitoTracker Green can stain mitochondria regardless of mitochondrial potential. TMRM (red) was used as the marker of mitochondrial potential. Nuclei were labeled by Hoechst (blue). In addition, the mitochondrial and cytosolic (without mitochondria) fractions of HUVECs treated with UV for 30 min, untreated HUVECs or HUVECs treated with 1 μM rISM for indicated period of time were isolated as previously described. WB was used to detect the release of proapoptotic factors- cytochrome *c* and AIF from mitochondria to cytoplasm owing to the loss of the mitochondrial potential. β-actin was used as the marker for cytoplasm. VDAC was used the marker for mitochondria.

Proximity ligation assay. HUVECs were incubated for 3 h in 2% FBS media with or without 1 μM rISM. The direct interactions between ISM and GRP78, ISM and integrin αvβ5, GRP78 and integrin αvβ5 were determined by the red PLA signals from Duolink *In Situ* (Olink Bioscience, Uppsala, Sweden).

Statistical analysis. Data were expressed as mean ± S.E.M. Statistical significance was determined using ANOVA. $^{*}P<0.05$; $^{**}P<0.01$, $n>3$.

Conflict of Interest

The authors declare no conflict of interest.

Acknowledgements. We thank Professor RM Kini at the Department of Biological Sciences and Dr. Yu-Chin Su at the Department of Pharmacy, National University of Singapore for their helpful discussions. This work is sponsored by grants from the Singapore Biomedical Research Council (BMRC07/1/21/19/493) and Ministry of Education (R-154-000-516-112) to RG and Singapore National Medical Research Council (NMRC/1317/2011) to VCY.

1. Carmeliet P. Angiogenesis in life, disease and medicine. *Nature* 2005; **438**: 932–936.
2. Folkman J. Role of angiogenesis in tumor growth and metastasis. *Semin Oncol* 2002; **29**(Suppl 16): 15–18.
3. Xiang W, Ke Z, Zhang Y, Ho-Yuet Cheng G, Irwan ID, Sulochana KN *et al.* Isthmin is a novel secreted angiogenesis inhibitor that inhibits tumour growth in mice. *J Cell Mol Med* 2011; **15**: 359–374.
4. Pera EM, Kim JI, Martinez SL, Brechner M, Li SY, Wessely O *et al.* Isthmin is a novel secreted protein expressed as part of the Fgf-8 synexpression group in the Xenopus midbrain-hindbrain organizer. *Mech Dev* 2002; **116**: 169–172.
5. Zhang Y, Chen M, Venugopal S, Zhou Y, Xiang W, Li YH *et al.* Isthmin exerts pro-survival and death-promoting effect on endothelial cells through alphavbeta5 integrin depending on its physical state. *Cell Death Dis* 2011; **2**: e153.
6. Davidson DJ, Haskell C, Majest S, Kherzai A, Egan DA, Walter KA *et al.* Kringle 5 of human plasminogen induces apoptosis of endothelial and tumor cells through surface-expressed glucose-regulated protein 78. *Cancer Res* 2005; **65**: 4663–4672.
7. Burikhanov R, Zhao Y, Goswami A, Qiu S, Schwarze SR, Rangnekar VM. The tumor suppressor Par-4 activates an extrinsic pathway for apoptosis. *Cell* 2009; **138**: 377–388.
8. Lee AS. GRP78 induction in cancer: therapeutic and prognostic implications. *Cancer Res* 2007; **67**: 3496–3499.
9. Schwarze S, Rangnekar VM. Targeting plasma membrane GRP78 for cancer growth inhibition. *Cancer Biol Ther* 2010; **9**: 153–155.
10. Sato M, Yao VJ, Arap W, Pasqualini R. GRP78 signaling hub a receptor for targeted tumor therapy. *Adv Genet* 2010; **69**: 97–114.
11. Arap MA, Lahdenranta J, Mintz PJ, Hajitou A, Sarkis AS, Arap W *et al.* Cell surface expression of the stress response chaperone GRP78 enables tumor targeting by circulating ligands. *Cancer Cell* 2004; **6**: 275–284.
12. Miao YR, Eckhardt BL, Cao Y, Pasqualini R, Argani P, Arap W *et al.* Inhibition of established micrometastases by targeted drug delivery via cell surface-associated GRP78. *Clin Cancer Res* 2013; **19**: 2107–2116.
13. Rasche L, Duell J, Morgner C, Chatterjee M, Hensel F, Rosenwald A *et al.* The natural human IgM antibody PAT-SM6 induces apoptosis in primary human multiple myeloma cells by targeting heat shock protein GRP78. *PLoS One* 2013; **8**: e63414.
14. Le Roy C, Wrana JL. Clathrin- and non-clathrin-mediated endocytic regulation of cell signalling. *Nat Rev Mol Cell Biol* 2005; **6**: 112–126.
15. Ivanov AI. Pharmacological inhibition of endocytic pathways: is it specific enough to be useful? *Methods Mol Biol* 2008; **440**: 15–33.
16. Chen Y, Wang S, Lu X, Zhang H, Fu Y, Luo Y. Cholesterol sequestration by nystatin enhances the uptake and activity of endostatin in endothelium via regulating distinct endocytic pathways. *Blood* 2011; **117**: 6392–6403.
17. Mousavi SA, Malerod L, Berg T, Kjeken R. Clathrin-dependent endocytosis. *Biochem J* 2004; **377**(Pt 1): 1–16.
18. Pfaffenbach KT, Lee AS. The critical role of GRP78 in physiologic and pathologic stress. *Curr Opin Cell Biol* 2011; **23**: 150–156.
19. Hendershot L. The ER function BiP is a master regulator of ER function. *Mt Sinai J Med* 2004; **71**: 289–297.
20. Ni M, Zhang Y, Lee AS. Beyond the endoplasmic reticulum: atypical GRP78 in cell viability, signalling and therapeutic targeting. *Biochem J* 2011; **434**: 181–188.
21. Lee A. GRP78 induction in cancer: therapeutic and prognostic implications. *Cancer Res* 2007; **67**: 3496–3499.
22. Berger C, Dong Z, Hanlon D, Bisaccia E, Edelson R. A lymphocyte cell surface heat shock protein homologous to the endoplasmic reticulum chaperone, immunoglobulin heavy chain binding protein BIP. *Int J Cancer* 1997; **71**: 1077–1085.
23. Zhang Y, Liu R, Ni M, Gill P, Lee AS. Cell surface relocalization of the endoplasmic reticulum chaperone and unfolded protein response regulator GRP78/BiP. *J Biol Chem* 2010; **285**: 15065–15075.
24. Yoshioka T, Nishikawa Y, Ito R, Kawamata M, Doi Y, Yamamoto Y *et al.* Significance of integrin alphavbeta5 and erbB3 in enhanced cell migration and liver metastasis of colon carcinomas stimulated by hepatocyte-derived heregulin. *Cancer Sci* 2010; **101**: 2011–2018.
25. Fiore C, Trezeguet V, Le Saux A, Roux P, Schwimmer C, Dianoux AC *et al.* The mitochondrial ADP/ATP carrier: structural, physiological and pathological aspects. *Biochimie* 1998; **80**: 137–150.
26. Palmieri F. The mitochondrial transporter family (SLC25): physiological and pathological implications. *Pflugers Arch* 2004; **447**: 689–709.
27. Dolce V, Scarcia P, Iacopetta D, Palmieri F. A fourth ADP/ATP carrier isoform in man: identification, bacterial expression, functional characterization and tissue distribution. *FEBS Lett* 2005; **579**: 633–637.
28. Wu C, Orozco C, Boyer J, Leglise M, Goodale J, Batalov S *et al.* BioGPS: an extensible and customizable portal for querying and organizing gene annotation resources. *Genome Biol* 2009; **10**: R130.
29. Su AI, Wiltshire T, Batalov S, Lapp H, Ching KA, Block D *et al.* A gene atlas of the mouse and human protein-encoding transcriptomes. *Proc Natl Acad Sci USA* 2004; **101**: 6062–6067.
30. Su AI, Cooke MP, Ching KA, Hakak Y, Walker JR, Wiltshire T *et al.* Large-scale analysis of the human and mouse transcriptomes. *Proc Natl Acad Sci USA* 2002; **99**: 4465–4470.
31. Lieberthal W, Menza SA, Levine JS, Graded ATP. depletion can cause necrosis or apoptosis of cultured mouse proximal tubular cells. *Am J Physiol* 1998; **274**(Pt 2): F315–F327.
32. Feldenberg LR, Thevananther S, del Rio M, de Leon M, Devarajan P. Partial ATP depletion induces Fas- and caspase-mediated apoptosis in MDCK cells. *Am J Physiol* 1999; **276**(Pt 2): F837–F846.
33. Galluzzi L, Vitale I, Abrams JM, Alnemri ES, Baehrecke EH, Blagosklonny MV *et al.* Molecular definitions of cell death subroutines: recommendations of the Nomenclature Committee on Cell Death 2012. *Cell Death Differ* 2012; **19**: 107–120.

34. Soderberg O, Gullberg M, Jarvius M, Ridderstrale K, Leuchowius KJ, Jarvius J *et al.* Direct observation of individual endogenous protein complexes in situ by proximity ligation. *Nat Methods* 2006; **3**: 995–1000.
35. Rapaport D. How does the TOM complex mediate insertion of precursor proteins into the mitochondrial outer membrane? *J Cell Biol* 2005; **171**: 419–423.
36. Lister R, Hulett JM, Lithgow T, Whelan J. Protein import into mitochondria: origins and functions today (review). *Mol Membr Biol* 2005; **22**: 87–100.
37. Lee TY, Muschal S, Pravda EA, Folkman J, Abdollahi A, Javaherian K. Angiostatin regulates the expression of antiangiogenic and proapoptotic pathways via targeted inhibition of mitochondrial proteins. *Blood* 2009; **114**: 1987–1998.
38. Rehn M, Veikkola T, Kukk-Valdre E, Nakamura H, Ilmonen M, Lombardo C *et al.* Interaction of endostatin with integrins implicated in angiogenesis. *Proc Natl Acad Sci USA* 2001; **98**: 1024–1029.
39. Chandrasekaran L, He CZ, Al-Barazi H, Krutzsch HC, Iruela-Arispe ML, Roberts DD. Cell contact-dependent activation of alpha3beta1 integrin modulates endothelial cell responses to thrombospondin-1. *Mol Biol Cell* 2000; **11**: 2885–2900.
40. Mikhailenko I, Krylov D, Argraves KM, Roberts DD, Liau G, Strickland DK. Cellular internalization and degradation of thrombospondin-1 is mediated by the amino-terminal heparin binding domain (HBD). High affinity interaction of dimeric HBD with the low density lipoprotein receptor-related protein. *J Biol Chem* 1997; **272**: 6784–6791.
41. Kumar S, Sharghi-Namini S, Rao N, Ge R. ADAMTS5 functions as an anti-angiogenic and anti-tumorigenic protein independent of its proteoglycanase activity. *Am J Pathol* 2012; **181**: 1056–1068.
42. Manders EM, Stap J, Brakenhoff GJ, van Driel R, Aten JA. Dynamics of three-dimensional replication patterns during the S-phase, analysed by double labelling of DNA and confocal microscopy. *J Cell Sci* 1992; **103**(Pt 3): 857–862.
43. Costes SV, Daelemans D, Cho EH, Dobbin Z, Pavlakis G, Lockett S. Automatic and quantitative measurement of protein-protein colocalization in live cells. *Biophys J* 2004; **86**: 3993–4003.
44. Manders EMM, Verbeek FJ, Aten JA. Measurement of co-localization of objects in dual color confocal images. *J Microsc* 1993; **169**(Pt 3): 375–382.
45. Casavan W, Gaidoukevitch Y, Parry-Hill MJ, Claxton NS, Davidson MW. Colocalization of fluorophores in confocal microscopy. In: *Olympus Interactive Java Tutorials* 2004. Available from http://www.olympusmicro.com/primer/java/colocalization/index.html.
46. Shi H, Huang Y, Zhou H, Song X, Yuan S, Fu Y *et al.* Nucleolin is a receptor that mediates antiangiogenic and antitumor activity of endostatin. *Blood* 2007; **110**: 2899–2906.
47. Pfeffer S, Brandt F, Hrabe T, Lang S, Eibauer M, Zimmermann R *et al.* Structure and 3D arrangement of endoplasmic reticulum membrane-associated ribosomes. *Structure* 2012; **20**: 1508–1518.
48. Watts C, Wickner W, Zimmermann R. M13 procoat and a pre-immunoglobulin share processing specificity but use different membrane receptor mechanisms. *Proc Natl Acad Sci USA* 1983; **80**: 2809–2813.
49. Nishiuchi R, Takagi J, Hayashi M, Ido H, Yagi Y, Sanzen N *et al.* Ligand-binding specificities of laminin-binding integrins: a comprehensive survey of laminin-integrin interactions using recombinant alpha3beta1, alpha6beta1, alpha7beta1 and alpha6beta4 integrins. *Matrix Biol* 2006; **25**: 189–197.

Supplementary Information accompanies this paper on Cell Death and Differentiation website (http://www.nature.com/cdd)